IEEE Access
Multidisciplinary | Rapid Review | Open Access Journal

Received January 13, 2021, accepted February 1, 2021, date of publication February 4, 2021, date of current version February 12, 2021.

Digital Object Identifier 10.1109/ACCESS.2021.3057084

Polarization Characteristics of the Near-Field Distribution of One-Dimensional Subwavelength Gratings

YUAN LI[1], JUNHONG SU[1], JUNQI XU[1], LIHONG YANG[1], DING CHEN[2], (Member, IEEE), AND GUOLIANG YANG[1]

[1]Shaanxi Province Key Laboratory of Thin Films Technology and Optical Test, Xi'an Technological University, Xi'an 710021, China
[2]School of Armament Science and Technology, Xi'an Technological University, Xi'an 710021, China

Corresponding author: Junhong Su (sujhong@126.com)

This work was supported by the National Natural Science Foundation of China under Grant 61378050.

ABSTRACT To improve the anti-laser damage performance of one-dimensional (1D) subwavelength gratings (SWGs), this paper proposes to reasonably reduce the peak electric field at the grating ridges to further reduce the laser damage caused by the electric field contribution. Based on Maxwell's equations, the equations for solving the field intensity of the near-field distribution of the dielectric materials are derived. The numerical simulation theoretical model is described. A 1064 nm laser in the –y direction irradiates the geometric surfaces under two perpendicular polarization directions: perpendicular to the grating ridges (transverse magnetic wave (TM) or x-polarization) and parallel to the grating ridges (transverse electric wave (TE) or z-polarization). We discuss the effects of the profile shape, structural parameters and refractive index of the material on the near-field distribution at the 1D SWG ridges by using a finite element method (FEM). The near-field distribution is sensitive to the x- and z-polarization of incident light. The near-field distribution of the 1D SWGs for TM waves is modulated by the surface, whereas that for TE waves is similar to the distribution of the bare substrate. The results show that the near-field distribution of 1D SWGs greatly depends on the laser polarization direction.

INDEX TERMS Dielectric materials, finite element method (FEM), near-field distribution, one-dimensional (1D) subwavelength gratings (SWGs), polarization direction.

I. INTRODUCTION

Subwavelength gratings (SWGs) are an effective substitute for laser thin films of optical elements used for high-power laser technology [1]. In recent years, SWGs have attracted great interest from scholars because of their good optical properties [1]–[3] and high laser-induced damage threshold (LIDT) [4], in which the LIDT is lower than that of the bare substrate but slightly higher than that of the multilayer film [5]. However, the resistance to laser damage of optical elements has been a limiting factor in the development of high-power laser systems. How to further improve the LIDT of optical elements is a constant pursuit of researchers in the development of high-energy laser systems. Many studies are being conducted to further improve the LIDT of optical elements. The field intensity distribution in and on the surface of optical elements has aroused great interest as one of the many factors that affect the anti-laser-induced damage performance of optical elements. The LIDT of optical elements can be further improved by optimizing the field intensity design [6]–[8]. Various subwavelength antireflective surfaces [9] inspired by the structure of biological eyes have been studied [10]. Du *et al.* [4], [5] studied the effect of the local electric field (E-field) on 1064 nm laser damage of rectangular gratings and 2D cylindrical SWGs on fused silica, and the temperature distribution resulting from the internal electric field may be the main reason behind the damage. Kong *et al.* [3] found that the near-field distribution of the SWG structure obtained by a finite-difference time-domain (FDTD) method exhibits a strong dependence on the surface period. Jin *et al.* [11] studied the near-field distribution characteristics of two typical defects in dielectric

The associate editor coordinating the review of this manuscript and approving it for publication was Xihua Zou.

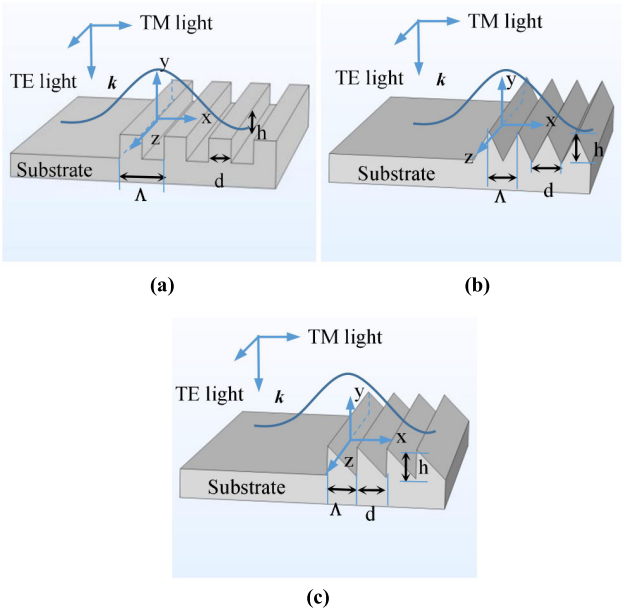

FIGURE 1. Schematic diagrams of the 1D SWG geometric models. (a) for the rectangular periodic grating. (b) for the isosceles triangular periodic grating. (c) for the right triangular periodic grating. The nomenclature for the geometric model dimensions is as follows: d is the grating bar width, Λ is the grating period, h is the grating height, and k is the propagation direction of the incident beam. The 1D SWGs have periodicity $\Lambda < \lambda$.

multilayer gratings (MDGs) using the Fourier model method. The study showed that the defects had little influence on the optical properties, but they may produce large changes in the internal electric field distribution on the grating surface and even in multilayer structures, thus decreasing the damage threshold of MDGs [11]. Gallais *et al.* [12] demonstrated that the laser damage characteristics of grating waveguides are well correlated with field enhancement. Jing *et al.*'s [13] study on the characteristics of femtosecond pulse breakdown in a sinusoidal SWG showed that the near-field distribution associated with the laser damage resistance ability strongly depends on the polarization state of incident light.

In this paper, the near-field distribution of geometric models irradiated by a 1064 nm nanosecond pulse laser is simulated by using finite element simulation software. The effects of different polarization states and structural parameters on the field intensity distribution are investigated in detail. This provides inspiration for further improving the anti-laser damage ability of SWGs.

II. THEORY

A. THEORETICAL MODEL

We propose a geometric model in which one half of the surface is an SWG and the other half is a bare substrate. The geometric model is used to intuitively analyze the field intensity distribution of the one-dimensional (1D) SWG surface relative to that of the bare substrate. Schematic diagrams of the geometric models with different shapes are shown in Fig. 1, where h, d, and Λ represent the height, bar width, and SWG period, respectively. The cross-section of the geometric models lies in the x-y plane and has a grating period Λ along the x direction.

The incident and outgoing materials for the Gaussian beam are air and the substrate, respectively. The wave vector of the Gaussian beam is *k*. The Gaussian beam is perpendicularly incident on the surface of the model, and the propagation direction is the –y direction. The focal plane is spanned by the x and z coordinates, and the waist of the Gaussian beam is located on the upper surface of the optical substrate, with the center at the origin of the coordinates. The size of the substrate is much larger than the diameter of the Gaussian spot, ensuring that the spot is on the substrate. The TE wave has the electric field component in the z direction, out of the modeling x-y plane, which is parallel to the grating ridges, that is, z-polarization. When the beam is polarized in the x direction, the electric field component is perpendicular to the grating ridges, that is, the TM wave or x-polarization.

In this paper, n_0 and n_s represent the refractive indices of the surrounding medium and the material, respectively, and the absorption coefficient and extinction coefficient of the dielectric material are ignored.

B. SOLUTION EQUATION OF THE NEAR-FIELD DISTRIBUTION

A laser beam consists of electromagnetic waves that satisfy Maxwell's equations. Therefore, the solution equations can be obtained in the frequency domain from Maxwell's equations, and the governing equation can be written in the form

$$\nabla \times \mu_r^{-1}(\nabla \times \boldsymbol{E}) - k_0^2 \varepsilon_r \boldsymbol{E} = 0 \tag{1}$$

for the time-harmonic problem. Here, $\boldsymbol{\varepsilon}_r$ is the relative permittivity and $\boldsymbol{\mu}_r$ is the relative permeability of the material. The wavenumber of free space k_0 is defined as

$$k_0 = \omega\sqrt{\varepsilon_0 \mu_0} = \frac{\omega}{c_0} \tag{2}$$

Using the relation $\boldsymbol{\varepsilon}_r = \boldsymbol{n}^2$, where $\boldsymbol{n}$ is the refractive index, the assumption is that the relative permittivity is $\boldsymbol{\mu}_r = 1$ and the electrical conductivity is $\sigma = 0$ for linear materials, and the equation can alternatively be written as

$$\nabla \times (\nabla \times \boldsymbol{E}) - k_0^2 n^2 \boldsymbol{E}0 \tag{3}$$

Various forms of laser polarization can be characterized by corresponding linear polarization states. This paper mainly analyzes the laser beam vertically incident with linearly polarized light. The incident plane is the xoy coordinate plane, the polarization in the x-axis direction is x-polarization, and the polarization perpendicular to the incident plane is z-polarization. When the geometric model exists, the incident field is the background field and the scattering field is the relative field in Maxwell's equations. In other words, when the geometric model exists, the field generated by the incident Gaussian beam is a scattering field. However, the electric or magnetic fields in Maxwell's equations are total fields. When the background electromagnetic field $\boldsymbol{E}_{\boldsymbol{background}}$ is given, which interacts with various

materials and structures, the objective is to obtain the total field $\boldsymbol{E_{total}}$ and the scattering field $\boldsymbol{E_{scattered}}$ by solving the following equations.

$$\nabla \times (\nabla \times \boldsymbol{E_{total}}) - k_0^2 n^2 \boldsymbol{E_{total}} = 0$$
$$\boldsymbol{E_{total}} = \boldsymbol{E_{background}} + \boldsymbol{E_{scattered}} \quad (4)$$

C. PLANE WAVE EXPRESSION OF A GAUSSIAN BEAM

The plane wave expansion formula is a more general and more accurate Gaussian beam formula. The plane wave expansion method is used to approximate the Gaussian beam in the focal plane to ensure the accuracy of the calculation. The wavelength of the Gaussian beam is 1064 nm, and the waist radius w_0 is 10.64 μm.

$$\boldsymbol{E}_{b,Gauss}(\boldsymbol{r}) = \boldsymbol{E}_0 \exp(-\frac{x^2+z^2}{w_0^2})\boldsymbol{e} = \sum_{l=-L}^{L}\sum_{m=-M}^{M}\sum_{j=0}^{1} a_{lmj}\boldsymbol{u}_j(\boldsymbol{k}_{lm}) \exp(-i\boldsymbol{k}_{lm}.\boldsymbol{r}) \quad (5)$$

where the beam is propagating in the negative y direction, the focal plane is spanned by the x and z coordinates, $\boldsymbol{e}$ is the unit magnitude transverse polarization in the focal plane, l and m denote the indices for the wave vectors, index j accounts for the two polarizations per wave vector $\boldsymbol{k}_{lm}$, α_{lmj} is the amplitude, $\boldsymbol{u}_j(\boldsymbol{k}_{lm})$ is the unit magnitude polarization, and $\boldsymbol{r}$ is the position vector. This method is based on the angular spectrum of plane waves [14].

Multiplying the above with the conjugate of the exponential factor and the polarization factor $\boldsymbol{u}_j(\boldsymbol{k}_{lm})$ and applying a surface integral over the entire focal plane, the amplitudes are extracted as

$$a_{lmj} = \frac{\boldsymbol{E}_0 w_0^2 (\boldsymbol{e} \cdot \boldsymbol{u}_j(\boldsymbol{k}_{lm}))}{4\pi} \exp(-\frac{\boldsymbol{k}_{t,lm}^2 w_0^2}{4}) \quad (6)$$

where $\boldsymbol{k}_{t,lm}$ is the magnitude of the transverse wave vector component and $\boldsymbol{E}_0$ is the normalized incident electric field.

III. POLARIZATION EFFECT ON THE NEAR-FIELD DISTRIBUTION AND DISCUSION

The influence of the SWG surface on the near-field distribution is analyzed by finite element simulation software. The normalized field intensity of the three different shapes of the SWG surface is simulated with the same structural parameters. One of the main reasons for the laser-induced damage to an SWG is the strong surface electric field distribution [4], [7], [11], [12], and the damage mainly occurs at the interface between the substrate and air [4]. For nanosecond laser-induced damage of optical dielectric materials, the material damage mechanisms, including avalanche ionization (AI) and photoionization (PI), are commonly accepted to contribute to material ablation, in which the heat conduction effect caused by nanosecond pulses can be negligible due to the significantly shorter time scale for electron energy transfer to the lattice [15], [16].

A critical electron density (CED) is used to identify the onset of material damage with nanosecond laser irradiation. An evolution equation for the electron density describes the PI and AI processes in a dielectric medium exposed to intense laser radiation [13]. The quantitative electric field ratio $|E/E_0|$, which is defined as the ratio of the internal field E in the microstructure to the incident field E_0, is shown in the near-field distribution images. The factor $|E/E_0|$ introduced into the evolution equation for the electron density represents the maximum electric field enhancement inside the investigated SWGs [13]. Therefore, we focus on the maximum peak electric field intensity of the near-field distribution at the grating layer.

In this paper, the effects of defects and material absorption and extinction coefficients are not considered. The refractive indices $n_0 = 1$ and $n_s = 1.52$ are used as the refractive indices of the surrounding medium and substrate, respectively, except for when discussing the effect of the refractive index on the near-field distribution of 1D SWGs.

A. EFFECT OF THE GRATING SHAPE ON THE NEAR-FIELD DISTRIBUTION

The distribution of the electric field varies with the surface shape when the laser irradiates the surface of an SWG, and the LIDT of the grating is related to the distribution of the electric field intensity [1], [3]. To objectively evaluate the electric field distribution of different gratings, the same grating parameters are used, and the normalized field intensity distribution is obtained.

The amplitude of the incident Gaussian beam is normalized, and the waist radius of the Gaussian beam is 10 times the wavelength of 1064 nm. The electric field distributions of the three different geometric models are simulated by finite element analysis (FEA). Higher-order diffraction orders, which exist as evanescent waves in the near-field region, make an important contribution to the electric field distribution [17]. The grating height and the period are 100 nm, and the ridge width d of the three gratings is 50 nm at z = 0. As mentioned above, laser-induced damage tends to occur at the interface between air and the medium, so the field intensity distributions on the surfaces of the three nanostructures are compared. Since various forms of laser polarization can be characterized by corresponding linear polarization states, two special cases of perpendicular laser incidence, namely, x-polarization and z-polarization, are discussed.

Fig. 2 shows the normalized near-field distributions of the 1D SWGs. As seen from the plots, half of the Gaussian beam is vertically incident on the SWG structure and the other on the flat substrate. In the configurations in the left column of Fig. 2, the Gaussian beam is polarized in the x direction (x-polarization), that is, in the direction of the grating vector. For this polarization, the electric field distribution of the Gaussian beam is modulated by the subwavelength surface. According to the local near-field magnification (Fig. 2. (a), (c), (e)), the stronger field intensity is distributed in the valleys on the surface of the nanostructure,

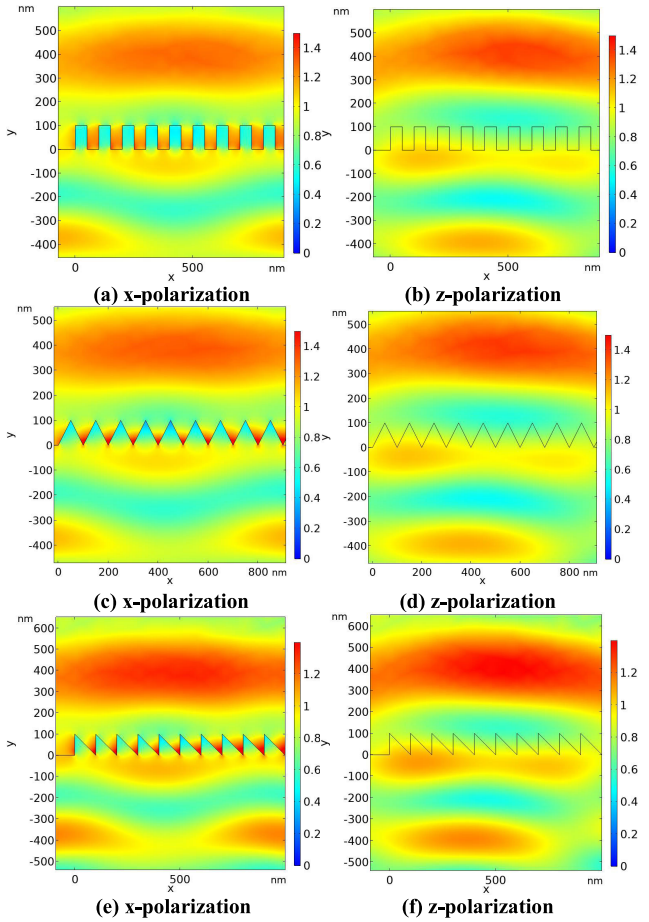

FIGURE 2. Normalized near-field distribution with an incident wavelength of 1064 nm for a period of 100 nm and a height of 100 nm at normal incidence. (a), (c), and (e) for x-polarization. (b), (d), and (f) for z-polarization. The W/Λ ratio of the rectangular SWGs is 0.5.

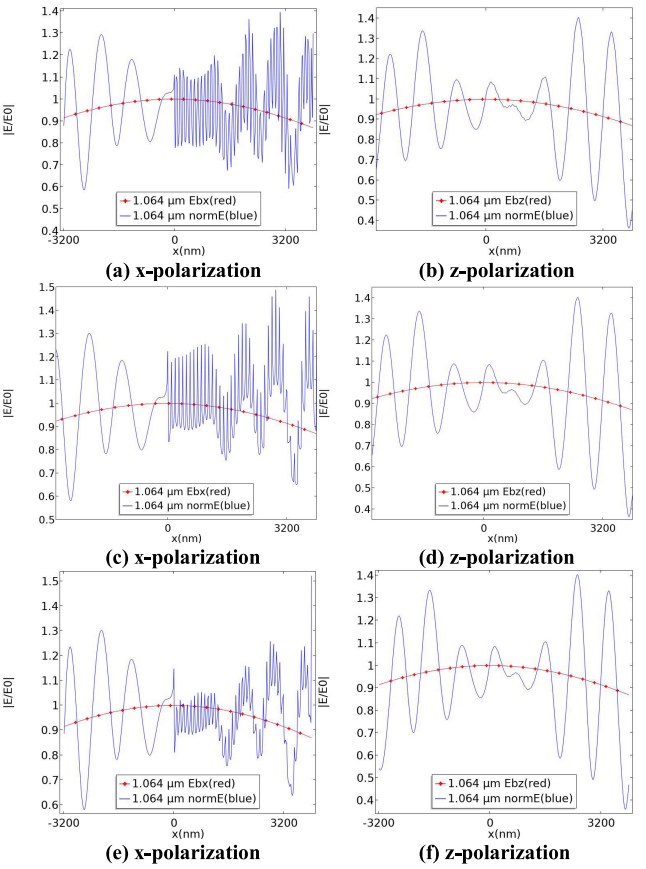

FIGURE 3. Line plots of the x or z component of the Gaussian beam background field (red line) and the electric field norm (blue line) at y = 0. (a) and (b) for the rectangular SWGs. (c) and (d) for the isosceles triangular SWGs. (e) and (f) for the right triangular SWGs. (a), (c), and (e) for x-polarization. (b), (d), and (f) for z-polarization.

which are areas surrounded by air. This is consistent with the results of Jin *et al*. [11].

When the beam is polarized along the grating ridge direction, that is, in the z direction (z-polarization), the electric field distribution of the Gaussian beam passing through the SWG structure is similar to that for the flat substrate, and no concentrated electric field enhancement occurs in the valleys on the surface of the nanostructure (Fig. 2. (b), (d), (f)). The results show that the near-field distribution of 1D SWGs is polarization dependent.

Fig. 3 shows two-dimensional (2D) cut lines of the normalized electric field amplitude of the 1D gratings at y = 0. The red curve represents the x component (Ebx) or z component (Ebz) of the Gaussian beam background field, and the blue line represents the electric field norm of the scattering field (normE).

For x-polarization, the periodic surface has a modulation effect on the field distribution. The field intensities of the three grating surfaces have the same frequency because they have the same grating period, but the peak intensities of the field intensity are different. The maximum electric field peak occurs at the interface between the grating surface and air. The peak intensity of the electric field on the surface of the right triangular grating is the lowest, while that of the isosceles triangular grating is the strongest. For z-polarization, the 2D cut line at y = 0 shows that the electric field norms of the three periodic surfaces are not significantly different, but the 1D SWG peaks are higher than those on the surface of the flat substrate. The frequency of the electric field oscillation is not modulated by the periodic surface nanostructures, which is different from x-polarization.

Figs. 2 and 3 show that the electric field distribution caused by the periodic shape of the surface of 1D SWGs is sensitive to the polarization direction. The rules are similar but the peak electric fields differ on the surfaces of the different-shaped SWGs, which may be the main reason why the 1D SWGs have different abilities to resist laser damage. Studying the parameters of 1D SWGs and the refractive indices is an effective way to analyze the law of the peak electric field near the grating ridges and thereby improve the LIDT of 1D SWGs.

B. EFFECT OF THE GRATING PERIOD ON THE NEAR-FIELD DISTRIBUTION

Figs. 4-6 show the 2D cut lines (y = 0) of the normalized electric field amplitude of the three geometric models:

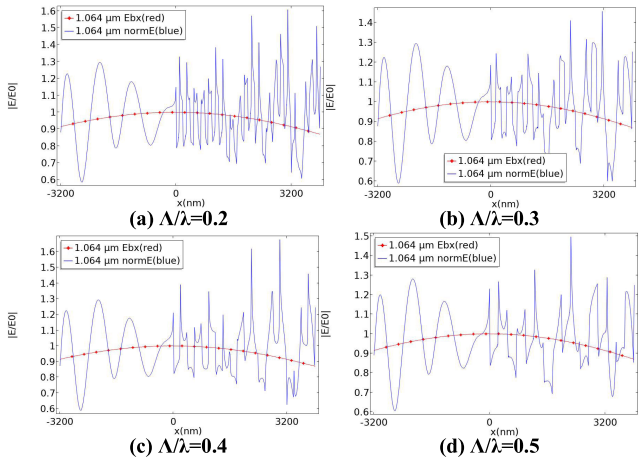

FIGURE 4. 2D cut line of the field intensity distribution on the surface of the 1D rectangular SWG at different periods. The beam is polarized in the x direction (x-polarization). The h/λ ratio is 0.1.

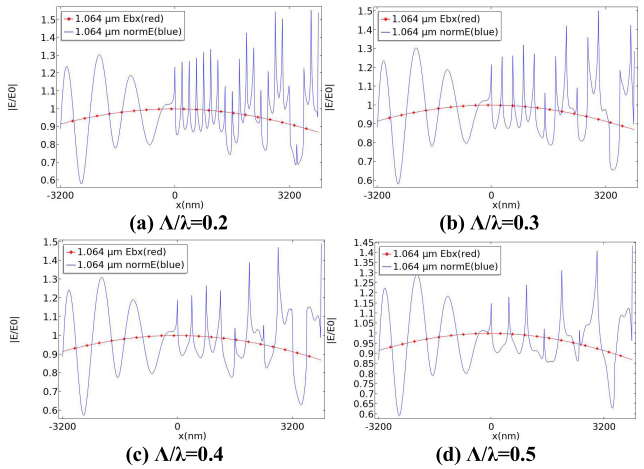

FIGURE 5. 2D cut line of the field intensity distribution on the surface of the 1D isosceles triangular SWG at different periods. The beam is polarized in the x direction (x-polarization). The h/λ ratio is 0.1.

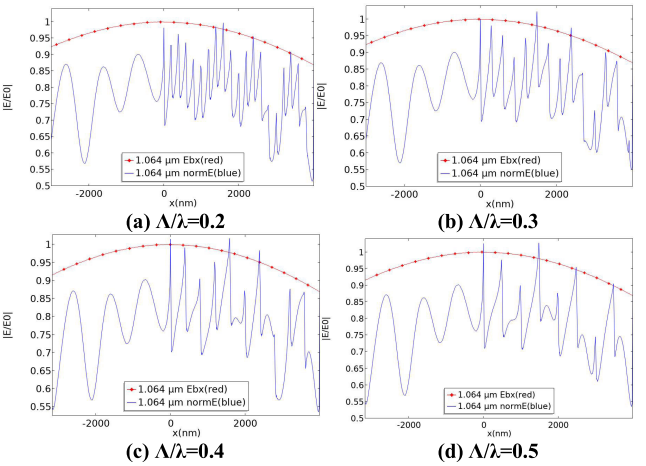

FIGURE 6. 2D cut line of the field intensity distribution on the surface of the 1D right triangular SWG at different periods. The beam is polarized in the x direction (x-polarization). The h/λ ratio is 0.1.

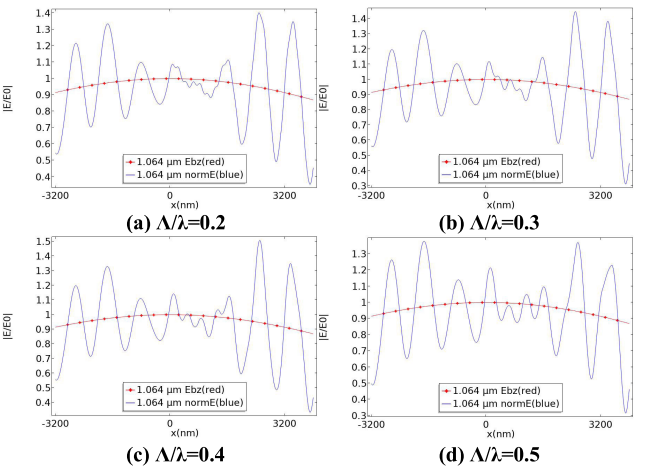

FIGURE 7. 2D cut line of the field intensity distribution on the surface of the 1D rectangular SWG at different periods. The beam is polarized in the z direction (z-polarization). The h/λ ratio is 0.1.

rectangular grating, isosceles triangular grating, and right triangular grating, respectively. The beam is polarized in the x direction (x-polarization). Figs. 7-9 show the 2D cut lines ($y = 0$) of the three geometric models for polarization in the z direction (z-polarization). The red curve represents the x component (**Ebx**) or z component (**Ebz**) of the Gaussian beam background field, and the blue line represents the electric field norm of the scattering field (**normE**). In Figs. 4-9, the right half ($x>0$) of each graph shows the electric field distribution caused by the surface of the periodic structure, while the left half ($x<0$) shows that caused by the bare substrate. The Λ/λ ratios of the 1D SWGs are 0.2, 0.3, 0.4, and 0.5. The h/λ ratio is 0.1.

For x-polarization, compared to the bare substrate, the electric field distribution caused by the surface of the periodic structure shows a fluctuation related to the period. The oscillation frequency of the peak field intensity is also related to the period. The shorter the period is, the higher the frequency of the electric field oscillation and the higher the peak density (the number of peaks per unit length) (Figs. 4-6). The maximum peak electric field induced by the three gratings is obviously higher than that induced by the bare substrate. However, for z-polarization, no periodic characteristic of the electric field distribution is induced by the periodic structure. This is different from the case of x-polarization (Figs. 7-9). The results show that the Λ/λ ratios of 1D SWGs affect the peak density of the field distribution along with the polarization direction of the incident light.

C. EFFECT OF THE GRATING HEIGHT ON THE NEAR-FIELD DISTRIBUTION

To study the influence of the height of the SWG on the near-field distribution, several key grating heights h, $h = 0.1\lambda$, $h = 0.5\lambda$, and $h = \lambda$, should be considered at the same grating period. However, in practice, the grating height cannot be increased indefinitely due to the influence of the fabrication process [11]. When the height changes, the field distributions caused by the surface structure of the three geometric models

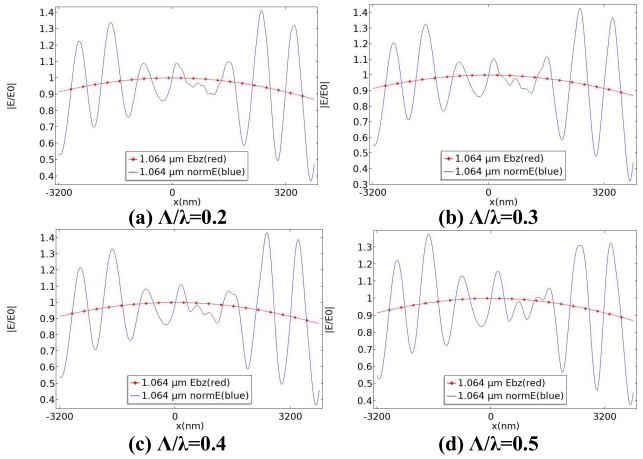

FIGURE 8. 2D cut line of the field intensity distribution on the surface of the 1D isosceles triangular SWG at different periods. The beam is polarized in the z direction (z-polarization). The h/λ ratio is 0.1.

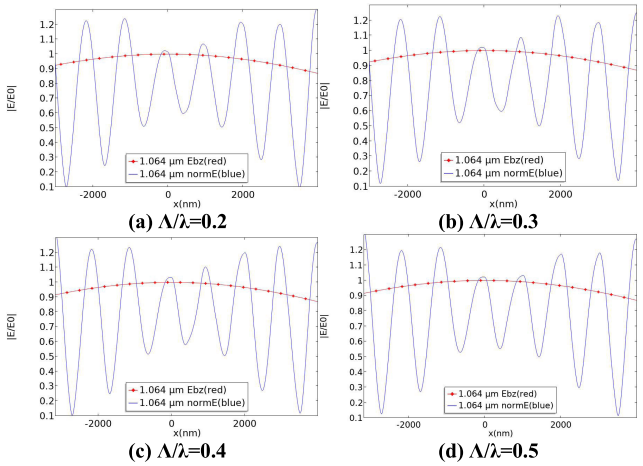

FIGURE 9. 2D cut line of the field intensity distribution on the surface of the 1D right triangular SWG at different periods. The beam is polarized in the z direction (z-polarization). The h/λ ratio is 0.1.

all present similar laws, so two of them are omitted here. We take the model with a low peak electric field as an example to analyze the effect of the grating height on the near-field distribution.

Fig. 10 shows the plots of the field intensity distribution of the geometric model (x>0) of the 1D right triangular SWG. For x-polarization, a superimposed peak electric field exists in the air gaps between the nanostructures. For z-polarization, the field superposition is not discretized by the periodic structures of the 1D SWG in the x direction. The maximum peak electric field appears at the grating ridges. These positions are often the source of laser damage caused by electric fields.

Fig. 11 shows the field strength distribution of the 1D right triangular geometric model. The h/λ ratios are 0.1, 0.5, and 1, and the Λ/λ ratio is 0.1. The right half of each graph (x>0) shows the electric field norm caused by the surface (y = 0) of the periodic structure. The left half shows that caused by the bare substrate. The left column is for

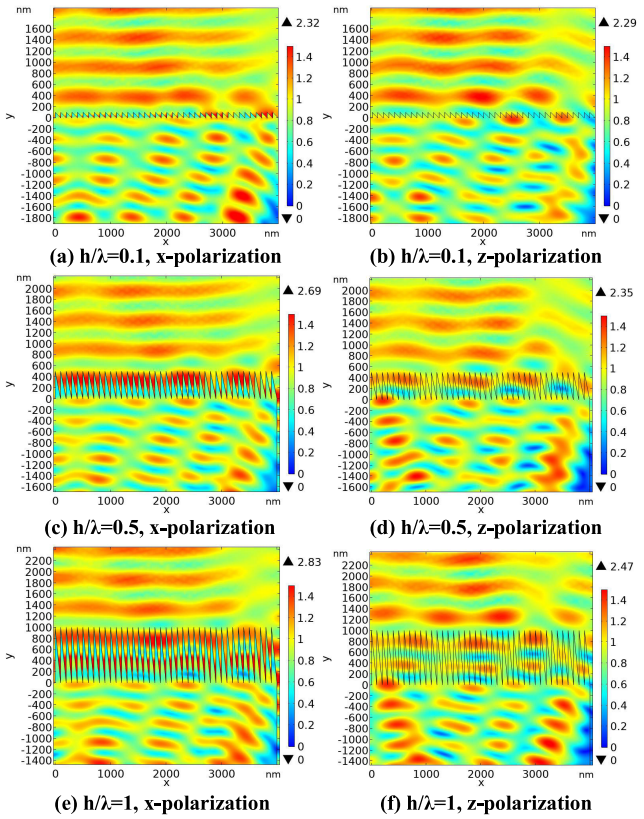

FIGURE 10. Plots of the field intensity distribution of the 1D right triangular SWG. The h/λ ratios are 0.1, 0.5 and 1, and the Λ/λ ratio is 0.1. (a), (c), and (e) for x-polarization. (b), (d), and (f) for z-polarization.

x-polarization, and the right column is for z-polarization. For x-polarization, the electric field distribution is modulated by the nanostructure, and the size of the sharp peaks is related to the height of the grating. As h/λ increases, the peak-valley value decreases. In contrast, the 1D SWG does not modulate the electric field for z-polarization. The larger h/λ is, the more the highest peak electric field moves toward the center of the beam.

D. EFFECT OF THE GRATING SUBSTRATE REFRACTIVE INDEX ON THE NEAR-FIELD DISTRIBUTION

To study the influence of the substrate refractive index on the near-field distribution of the 1D SWGs, different material refractive indices are investigated for the same structural parameters. Here, the h/λ ratio is 0.1, and the Λ/λ ratio is 0.2.

Fig. 12 shows the 2D cut lines of the field intensity distribution on the surface (y = 0) of the 1D right triangular SWG. The left column of Fig. 12 shows the 2D cut lines at y = 0 for x-polarization. The right column shows the 2D cut lines at y = 0 for z-polarization. In Fig. 12 a and b, the refractive index is 1.45. In Fig. 12 c and d, the refractive index is 1.52. In Fig. 12 e and f, the refractive index is 2.3. For x- and z-polarization, the larger the refractive index is, the larger the maximum peak electric field compared to the bare substrate.

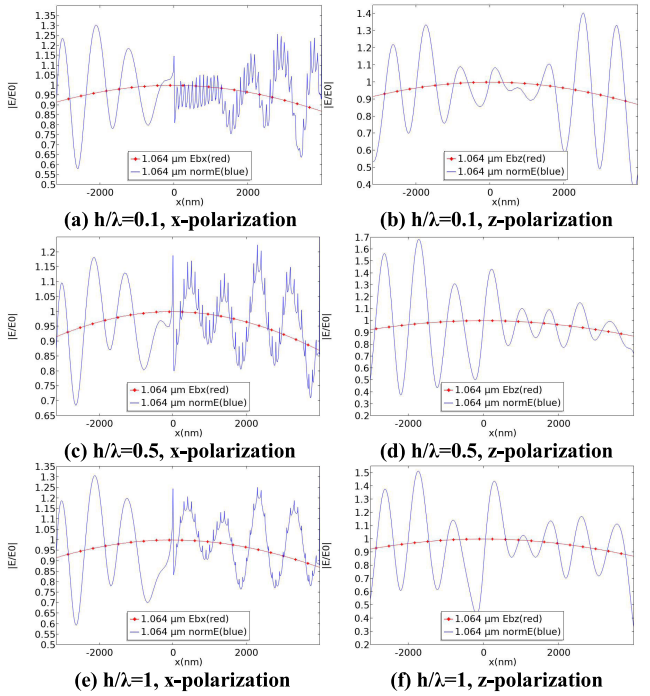

FIGURE 11. 2D cut line of the field intensity distribution of the 1D right triangular SWG at y = 0. The Λ/λ ratio is 0.1.

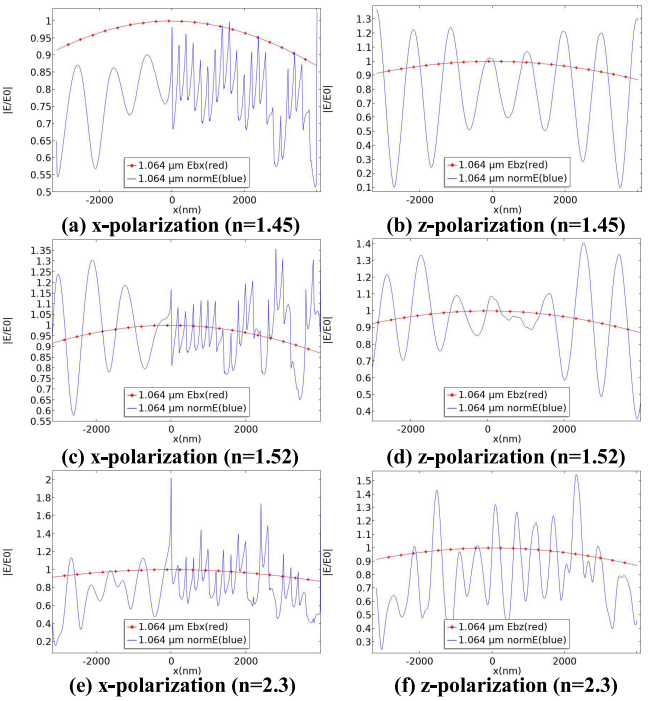

FIGURE 12. 2D cut line of the field intensity distribution on the surface (y = 0) of the 1D right triangular SWG for different refractive indices. The h/λ ratio is 0.1, and the Λ/λ ratio is 0.2. (a), (c), and (e) for x-polarization. (b), (d), and (f) for z-polarization.

IV. CONCLUSION

The anti-laser damage performance of a grating is related to the peak electric field at the ridges of the grating. By analyzing the near-field distribution of 1D SWGs, the variation law of the peak electric field is obtained, which provides inspiration for obtaining high LIDT SWGs.

We derive the governing equations in the frequency domain from Maxwell's equations and the constitutive relation. The background field is expressed by the plane wave expansion of the Gaussian beam to solve for the scattering field.

The near-field distribution of the geometric models irradiated by a 1064 nm laser is calculated by finite element simulation software. The normalized field distribution of the 1D SWGs for different grating periods, grating heights, and material refractive indices are simulated.

The results show that the peak field intensities of the electric field distribution caused by different periodic surface topographies are different. The normalized distribution of the electric field on the surface of the 1D SWGs is related to the polarization direction of incident light. When the beam is polarized in the x direction (x-polarization), a stronger field intensity is distributed in the valleys on the surface of the nanostructure, and the periodic surface has a modulation effect on the field distribution. The maximum electric field peak occurs at the interface between the grating surface and air, which is the origin of laser damage. In addition, the period of the peak electric field is the same as that of the grating, and as the h/λ ratio increases, the peak-valley value decreases. Without considering the absorption and extinction coefficients, the larger the refractive index of the material is, the greater the peak electric field induced by the nanoarray surface.

When the beam is polarized in the z direction (z-polarization), the near-field distribution induced by the 1D SWGs is similar to that induced by the bare substrate. The periodicity of the 1D SWGs does not affect the oscillation frequency or the peak number of the electric field. The refractive index still has a significant effect on the near-field distribution of the 1D SWGs. The higher the material refractive index is, the higher the peak intensity for the same other parameters.

Studies show that the peak electric field strength at the ridges induced by 1D SWGs can be further reduced by optimizing the grating shape, parameters or material according to the application. The results provide some references for further study of the laser damage properties of micro/nanostructured optical elements.

REFERENCES

[1] X. Ye, J. Huang, F. Geng, H. Liu, L. Sun, L. Yan, X. Jiang, W. Wu, and W. Zheng, "High power laser antireflection subwavelength grating on fused silica by colloidal lithography," *J. Phys. D, Appl. Phys.*, vol. 49, no. 26, May 2016, Art. no. 265104, doi: 10.1088/0022-3727/49/26/265104.

[2] X. Jing, J. Zhang, S. Jin, P. Liang, and Y. Tian, "Design of highly efficient transmission gratings with deep etched triangular grooves," *Appl. Opt.*, vol. 51, no. 33, pp. 7920–7933, Nov. 2012, doi: 10.1364/ao.51.007920.

[3] F. Kong, H. Huang, L. Wang, J. Shao, Y. Jin, Z. Xia, J. Chen, and L. Li, "Femtosecond laser induced damage of pulse compression gratings," *Opt. Laser Technol.*, vol. 97, pp. 339–345, Dec. 2017, doi: 10.1016/j.optlastec.2017.07.021.

[4] Y. Du, X. Wu, M. Zhu, and Z. Le, "Theoretical and experimental research on laser-induced damage of cylindrical subwavelength grating," *Opt. Exp.*, vol. 23, no. 19, pp. 24296–24307, Sep. 2015, doi: 10.1364/oe.23.024296.

[5] Y. Du, M. Zhu, Q. Liu, Z. Sui, K. Yi, Y. Jin, and H. He, "Laser-induced damage properties of subwavelength antireflective grating on fused silica," *Thin Solid Films*, vol. 567, pp. 47–53, Sep. 2014, doi: 10.1016/j.tsf.2014.07.028.
[6] C. Li, Q. Li, L. Sun, X. Ye, S. Chen, Z. Wu, J. Huang, W. Wu, and X. Jiang, "Effect of PVA coating on the electric field intensity distribution and laser damage performance of fused silica optics surfaces," *Opt. Exp.*, vol. 26, no. 15, pp. 19707–19717, Jul. 2018, doi: 10.1364/oe.26.019707.
[7] C. Li, Y. Zhao, Y. Cui, Y. Wang, X. Peng, C. Shan, M. Zhu, J. Wang, and J. Shao, "Investigation on picosecond laser-induced damage in HfO_2/SiO_2 high-reflective coatings," *Opt. Laser Technol.*, vol. 106, pp. 372–377, Oct. 2018, doi: 10.1016/j.optlastec.2018.04.028.
[8] Y. Chai, M. Zhu, H. Wang, H. Xing, Y. Cui, J. Sun, K. Yi, and J. Shao, "Laser-resistance sensitivity to substrate pit size of multilayer coatings," *Sci. Rep.*, vol. 6, no. 1, p. 27076, Jun. 2016, doi: 10.1038/srep27076.
[9] S. Chattopadhyay, Y. F. Huang, Y. J. Jen, A. Ganguly, K. H. Chen, and L. C. Chen, "Anti-reflecting and photonic nanostructures," *Mater. Sci. Eng., R, Rep.*, vol. 69, nos. 1–3, pp. 1–35, Jun. 2010, doi: 10.1016/j.mser.2010.04.001.
[10] Y. Li, J. Zhang, and B. Yang, "Antireflective surfaces based on biomimetic nanopillared arrays," *Nano Today*, vol. 5, no. 2, pp. 117–127, Apr. 2010, doi: 10.1016/j.nantod.2010.03.001.
[11] Y. Jin, H. Guan, F. Kong, J. Wang, A. Erdmann, S. Liu, Y. Du, J. Shao, H. He, and K. Yi, "Influence of two typical defects on the near-field optical properties of multilayer dielectric compression gratings," *Appl. Opt.*, vol. 51, no. 27, pp. 6683–6690, Sep. 2012, doi: 10.1364/ao.51.006683.
[12] L. Gallais, M. Rumpel, M. Moeller, T. Dietrich, T. Graf, and M. A. Ahmed, "Investigation of laser damage of grating waveguide structures submitted to sub-picosecond pulses," *Appl. Phys. B, Lasers Opt.*, vol. 126, no. 4, p. 69, Mar. 2020, doi: 10.1007/s00340-020-07419-2.
[13] X. Jing, Y. Tian, J. Han, J. Ma, Y. Jin, J. Shao, and Z. Fan, "Polarization effect of femtosecond pulse breakdown in subwavelength antireflective relief grating," *Opt. Commun.*, vol. 284, no. 18, pp. 4220–4224, Aug. 2011, doi: 10.1016/j.optcom.2011.04.058.
[14] M. Born and E. Wolf, *Principles of Optics*. Cambridge, U.K.: Cambridge Univ. Press, 1999, pp. 639–642.
[15] B. C. Stuart, M. D. Feit, S. Herman, A. M. Rubenchik, B. W. Shore, and M. D. Perry, "Nanosecond-to-femtosecond laser-induced breakdown in dielectrics," *Phys. Rev. B, Condens. Matter*, vol. 53, no. 4, pp. 1749–1761, Jan. 1996, doi: 10.1103/physrevb.53.1749.
[16] B. C. Stuart, M. D. Feit, A. M. Rubenchik, B. W. Shore, and M. D. Perry, "Laser-induced damage in dielectrics with nanosecond to subpicosecond pulses," *Phys. Rev. Lett.*, vol. 74, no. 12, pp. 2248–2251, Mar. 1995, doi: 10.1103/PhysRevLett.74.2248.
[17] S. Liu, Z. Shen, W. Kong, J. Shen, Z. Deng, Y. Zhao, J. Shao, and Z. Fan, "Optimization of near-field optical field of multi-layer dielectric gratings for pulse compressor," *Opt. Commun.*, vol. 267, no. 1, pp. 50–57, Nov. 2006, doi: 10.1016/j.optcom.2006.06.022.

YUAN LI was born in Weinan, Shaanxi, China, in 1982. She received the B.E. degree in optical engineering and the M.E. degree in microelectronics and solid-state electronics from Xi'an Technological University, China, in 2005 and 2011, respectively, where she is currently pursuing the Ph.D. degree in optical engineering.

Her research interests include anti-laser damage of micro- or nano-structured surfaces and optical materials.

Ms. Li's awards include the National Scholarship and an Assistant-Research Grant.

JUNHONG SU was born in Shaanxi, China, in 1963. He received the B.E. degree in optical measurement from the Xi'an Institute of Technology (now Xi'an Technological University), in 1984, and the M.E. and Ph.D. degrees in optical engineering from the Nanjing University of Science and Technology.

He is currently a Professor and a Ph.D. Supervisor with the Xi'an Technological University and the Director of the Shaanxi Key Laboratory of Photoelectric Test and Instrument Technology. He has published six translations and textbooks. Since 2008, he has published more than 100 papers as the first author. More than 70 of them have been included in SCI and EI. In addition, he holds 20 patents of various types. His research interests include optical detection technology of optoelectronic systems and devices, theoretical research and performance testing of optical films against laser damage, testing of laser parameters in high-intensity laser systems, and performance evaluation of systems and devices after interaction with photoelectric systems and devices.

As primary accomplishments, he won one project each of the second and third prizes of Science and Technology in Shaanxi Province, one project of the third prize of National Defense Science and Technology Progress, three projects of the third prize Of Ordnance Science and Technology, one project each of the first and second prizes of Shaanxi Provincial Science and Technology Progress, and two projects of the first prize of Shaanxi Provincial Institutions of higher learning science and technology.

JUNQI XU was born in Shaanxi, China, in 1973. He received the B.E. and M.E. degrees in optical engineering from Xi'an Technological University, in 1996 and 2004, respectively, and the Ph.D. degree from Northwestern Polytechnical University, in 2009.

From August 2004 to February 2005, he was a Visiting Scholar with Nagoya University. He is currently a Professor with Xi'an Technological University engaged in the research and development of thin film technology and testing, coating equipment and auxiliary instruments. He has published more than 60 articles in academic journals at home and abroad, including eight SCI and 20 EI articles. He holds five authorized invention patents and four utility model patents. His research interests include thin film and plasma technology, optical testing technology, and ion source development.

Prof. Xu won two projects of second prizes at the provincial and ministerial level and three projects of second prizes at the department and bureau level.

LIHONG YANG was born in 1974. She received the B.E. and M.E. degrees from Xi'an Technological University, in 1998 and 2005, respectively, and the Ph.D. degree from the Xi'an University of Technology, in 2009.

From June 2013 to July 2013, she was a Visiting Scholar with the University of Technology, Tampere, Finland. She is currently a Professor with Xi'an Technological University engaged in photoelectric testing research. She participated in the compilation of two textbooks. She has published 35 articles, many of which have been included in EI. She holds one licensed software copyright as the first inventor, one invention patent as the main inventor, one utility model patent, one software copyright, and three accepted invention patents as the main inventor.

Prof. Yang won two projects of second prizes at the provincial and ministerial level and one project of second prizes at the department and bureau level.

DING CHEN (Member, IEEE) was born in Xi'an, Shaanxi, China, in 1982. He received the B.S. degree in electrical and information engineering, the M.S. degree in weapon systems and utilization engineering, and the Ph.D. degree in optical engineering from Xi'an Technological University, China, in 2004, 2006, and 2020, respectively.

From 2004 to 2006, he was an Assistant Engineer with Xi'an North Electro-Optic Company Ltd. From 2009 to 2010, he was a Lecturer with the Department of Electrical and Information, Xi'an University of Technological. From 2010 to 2016, he was a Senior Engineer with the Radar Design and Research Institute, Xi'an Huang-he Electromechanical Company Ltd. Since 2020, he has been an Assistant Professor with the School of Armament Science and Technology, Xi'an Technological University. He is the author of more than 70 articles in Chinese or English. Accordingly, his two papers were published in the IEEE Proceedings of the two international conferences. His research interests include photoelectric measurement and instrument technology, photoelectric information processing and acquisition, and radar/EW system design, simulation and testing.

Dr. Chen is a Senior Member of the Chinese Institute of Electronics. He is also a member of SPIE, IET, and IEICE. He attended the 2018 IEEE International Conference on Mechatronics and Automation (ICMA 2018), Changchun, China, and the 2018 IEEE International Conference on Sensor Networks and Signal Processing (SNSP 2018), Xi'an, China. Specifically, he made an oral presentation at ICMA 2018, and a poster was presented at SNSP 2018. He was a Reviewer of *IET Signal Processing*, the American *Journal of Information Science and Technology*, Romania *Journal of Optoelectronics and Advanced Materials*, and *Chinese Journal of Ordnance Equipment Engineering*.

GUOLIANG YANG was born in Shaanxi, China, in 1979. He received the B.E. degree from Northwest University, in 2001, and the M.E. degree from Shaanxi Normal University, in 2006. He is currently pursuing the Ph.D. degree in optical engineering with Xi'an Technological University, China.

He has published nearly ten papers. His research interests include photoelectric testing, intelligent information processing, and pattern recognition.

Mr. Yang's awards include a National Scholarship and an assistant-research grant.